Bioelectrochemistry 152 (2023) 108428

Contents lists available at ScienceDirect

Bioelectrochemistry

journal homepage: www.journals.elsevier.com/bioelectrochemistry

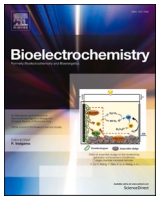

Haem-mediated albumin biosensing: Towards voltammetric detection of PFOA

Giulia Moro [a,b,c,*], Rui Campos [a,b,1], Elise Daems [a,b], Ligia Maria Moretto [c], Karolien De Wael [a,b]

[a] A-Sense Lab, University of Antwerp, Groenenborgerlaan 171, 2020 Antwerp, Belgium
[b] Nanolab Centre of Excellence, University of Antwerp, Groenenborgerlaan 171, 2020 Antwerp, Belgium
[c] Department of Molecular Sciences and Nanotechnologies, Ca' Foscari University of Venice, Via Torino 155, 30172 Venice, Italy

ARTICLE INFO

Keywords:
Albumin
Electrochemical biosensor
Hemin
Haem
PFOA
Perfluoroalkyl substances

ABSTRACT

The haem group is a promising redox probe for the design of albumin-based voltammetric sensors. Among the endogenous ligands carried by human serum albumin (hSA), haem is characterised by a reversible redox behaviour and its binding kinetics strongly depend on hSA's conformation, which, in turn, depends on the presence of other ligands. In this work, the potential applicability of haem, especially hemin, as a redox probe was first tested in a proof-of-concept study using perfluorooctanoic acid (PFOA) as model analyte. PFOA is known to bind hSA by occupying Sudlow's I site (FA7) which is spatially related to the haem-binding site (FA1). The latter undergoes a conformational change, which is expected to affect hemin's binding kinetics. To verify this hypothesis, hemin:albumin complexes in the presence/absence of PFOA were first screened by UV–Vis spectroscopy. Once the complex formation was verified, haem was further characterised via electrochemical methods to estimate its electron transfer kinetics. The hemin:albumin:PFOA system was studied in solution, with the aim of describing the multiple equilibria at stake and designing an electrochemical assay for PFOA monitoring. This latter could be integrated with protein-based bioremediation approaches for the treatment of per- and polyfluoroalkyl substances polluted waters. Overall, our preliminary results show how hemin can be applied as a redox probe in albumin-based voltammetric sensing strategies.

1. Introduction

Albumin-based electrochemical and optical sensors have shown promising results in the detection of metal ions [1,2], small molecules [3] as well as biomolecules [4]. Albumin, especially isoelectric bovine serum albumin (BSA), is a well-known blocking agent able to prevent non-specific adsorption phenomena in DNA/RNA sensors and immunosensors [5,6]. Lately, it has been largely applied in hybridised materials and in the formation of monolayers showing a high degree of compatibility with other biomolecules/bioreceptors (from peptides to DNA) [7,8]. The stability of albumins, especially BSA, in biosensing platforms was investigated considering variables such as temperature and light radiation [9]. The literature offers a rich background of experimental data, sensor design protocols and characterisation techniques for the application of albumin in electrochemical biosensors [10-13]. The electrochemical behaviour of both BSA and human serum albumin (hSA) was recorded on chemically modified screen-printed electrodes (SPEs) following the electrocatalytic oxidation of L-tyrosine and further applied in the label-free electroanalysis of protein-ligand interactions [14,15]. In the design of "*direct electrochemical strategies*" [16] based on hSA, we can include electroactive probes whose electrochemical behaviour can be easily recorded and correlated to the presence/absence of the hSA:analyte complex. Redox probes with an affinity lower than the ligand for hSA pockets can be loaded into the biorecognition layer [17]. Once loaded, these probes will show no electrochemical signal because they are *buried* in the hydrophobic pockets of hSA. When the ligand is present, the redox probe will be released. This event can be followed by recording the electrochemical response of the probe in solution, allowing an indirect, semi-quantitative detection of the ligand. Before considering designing *ad hoc* synthetic redox probes, naturally occurring and commercially available ones, such as hemin [18], should be tested. In this work, the use of hemin as a probe for the design of direct sensing strategies is evaluated.

Hemin [iron (III) protoporphyrin (IX) chloride] is a coordination

* Corresponding author at: A-Sense Lab, University of Antwerp, Groenenborgerlaan 171, 2020 Antwerp, Belgium.
E-mail address: giulia.moro@unive.it (G. Moro).
[1] Current address: Food Quality and Safety Group, International Iberian Nanotechnology Laboratory (INL), Av. Mestre José Veiga, 4715-330 Braga, Portugal.

https://doi.org/10.1016/j.bioelechem.2023.108428
Received 17 October 2022; Received in revised form 20 March 2023; Accepted 22 March 2023
Available online 27 March 2023

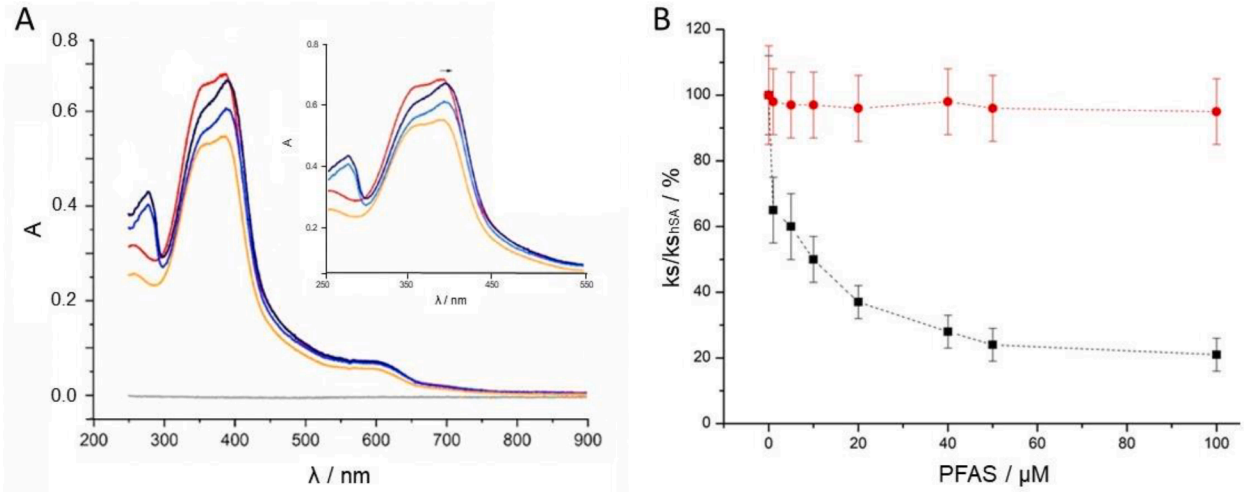

Figure 1. (**A**) UV–Vis absorption spectra of 10 μM hemin (H, red), 5:1 ratio hemin:hSA (H:hSA, navy blue), 5:1:50 ratio hemin:hSA:perflurooctanoic acid (H:hSA:PFOA, light blue) and negative control spectra of a 1:2 ratio hemin:PFOA (H:PFOA, orange) and 100 μM PFOA (PFOA, grey). Inset: the region between 250 and 550 nm with the Soret absorption band of hemin. (**B**) Overview of the data obtained in the kinetics study at different PFOA (black squares) and PFOS (red dots) concentrations. All measurements were carried out in triplicates and the average values with the associated errors are presented.

complex structurally equivalent to the prosthetic group of haemoglobins (*haem b*): it has a ferric centre (Fe^{3+}) coordinated with a tetradentate protoporphyrin ring and an axial chloride atom. The iron centre (Fe^{2+}/Fe^{3+}) of hemin is responsible for its electrochemical behaviour [18]. Endogenously produced in the human body, hemin can bind several proteins, such as hemopexin [19] and albumins (e.g., hSA) [20]. Artificial haemoproteins consisting of hSA:hemin complexes were synthesised to model globin-catalysed reactions [21,22]. In wild type hSA, the Fe^{3+} of the haem group coordinates with a histidine. Hemin, however, possesses a chloride ligand in the fifth coordination site of Fe^{3+} and is involved in binding interactions with serum proteins, such as albumins, to form methemalbumin [23].

Porphyrins show a poor water-solubility, thus the binding to serum proteins can increase their solubility [24]. According to Komatsu *et al.* [25], the features of the α-helical pockets of albumin are similar, in terms of hydrophobicity, to those of the haem-binding sites of haemoglobin and myoglobin. This structural similarity promotes hemin binding via hydrophobic interactions to the fatty acid site FA1 of hSA, which is a narrow D-shaped hydrophobic cavity located in subdomain IB (**Figure S1**) [26,27]. The central Fe^{3+} atom coordinates with the hydroxyl group of amino acid Y161 and the two-propionate groups are co-coordinated by three basic amino acid residues oriented towards the pocket entrance (R114, H146 and K190, inset **Figure S1**).

So far, hemin:albumin complexes have mainly been studied via crystallography, nuclear magnetic resonance, electron paramagnetic resonance, UV–Vis and fluorescence spectroscopy and electrochemistry [27-29]. The hemin:hSA binding results in a slight expansion of subdomain IB (i.e., a 1.4 Å separation increase in helices 8 and 10) which was also observed in the presence of fatty acids. Hemin binding does not alter hSA's conformation, but hemin's binding capability is dependent on the protein conformation and, therefore, on the presence of other ligands [25,30,31]. For instance, the binding of warfarin (WAR) and ibuprofen (IBU) to hSA's FA7 (Sudlow's drug-binding site I), located in the subdomain IIA, induces conformational changes (**Figure S2A**) able to affect haem transfer kinetics, increasing K_D values by one order of magnitude [30,32,33]. The correlation of these events is justified by the spatial proximity between FA1 (hemin cleft) and the WAR/IBU binding site [33]. Since the hemin:hSA binding kinetics could be affected by the conformational changes induced by the presence of WAR, hemin could possibly be used as an electroactive label in biosensing strategies for analytes binding to FA7 by recording the changes in its electrochemical behaviour.

FA7 was found to also entrap perfluorooctanoic acid (PFOA), a fluorinated manmade chemical that can be considered representative for the class of perfluoroalkyl substances (PFAS). Since their commercialisation in the late 1940s, PFAS have been found to be ubiquitous environmental pollutants and their harmful effects on animal and human health have been extensively investigated. Several toxicological studies described PFOA as a fatty acid mimic compound with a high affinity for serum carrier proteins, such as hSA [34,35]. The study of PFOA's binding mode described the formation of a 4:1 PFOA:hSA complex [35] and PFOA was observed to establish polar interactions in FA7 with the amino acid residues at the entrance of the pocket while its fluorinated tail accommodates within the hydrophobic region of the cavity.

PFOA binding was found to lead to the formation of a stable complex [36] and this feature was ascribed to PFOA's ability to compact hSA. These conformational changes were also observed via electrochemical impedance spectroscopy (EIS): hSA was immobilised on SPEs and the changes at the modified electrode/solution interface were considered to develop an impedimetric sensor for PFOA in water [37]. These findings can be used as a foundation for the design of other electrochemical sensing strategies. For instance, a voltammetric strategy correlating the changes in hemin's electrochemical signal intensity with PFOA levels, due to capability of PFOA to influence hemin:hSA binding, can be considered. Despite the complexity of the multiple equilibria at stake, the hemin signal is expected to increase with increasing concentrations of PFOA. Indeed, the equilibrium between hemin bound to hSA and hemin in solution will be shifted towards the latter since PFOA will alter hSA's conformation.

Aiming at verifying the above hypotheses, we designed this proof-of-concept study where, first, we monitored the influence of PFOA on the interaction between hemin and hSA via UV–Vis spectroscopy. Secondly, we studied the influence of PFOA on the hemin:hSA complex in solution. Hemin's electrochemical behaviour was characterised in aqueous solutions and its electron transfer constant was estimated using the Laviron formalism [38]. Thirdly, the hemin:hSA:PFOA system was applied as an hSA-based direct electrochemical sensing approach to detect PFOA by using hemin as a redox probe.

2. Materials and methods

2.1. Chemicals

Perfluorooctanoic acid (PFOA, ≥96%), perfluorooctanesulfonic acid

potassium salt (PFOS, ≥98%) and hemin (from bovine, ≥90%) were purchased from Sigma Aldrich Ltd (Belgium). A 0.1 M phosphate buffered saline (PBS) solution pH 7.4 with 0.01 M NaCl was prepared by mixing stock solutions of 0.1 M NaH_2PO_4 and 0.1 M Na_2HPO_4, purchased from Sigma Aldrich. All aqueous solutions were prepared using MilliQ water (R > 18 MΩ cm). Hemin stock solutions (from 1 to 5 mM) were prepared in DMSO or 100 mM NaOH, as specified afterwards, and diluted with PBS solution to reach DMSO/NaOH percentages lower than 2.5% in the tested solutions. Highly purified delipidated hSA was obtained by adsorption onto activated charcoal as described previously [39].

2.2. UV–Vis spectroscopy

The spectra were acquired in the UV–Vis region using an AvaLight-DH-S-BAL deuterium-halogen light source, coupled with an Avaspec-2048L detector (Avantes) with a 20 μm slit, using a fibre optics set-up. All measurements were recorded in 15 mL of 0.1 M PBS solution, using a 10 mm pathlength quartz cuvette (100-QS cuvette, Hellma Analytics) in oxygen-free conditions (30 min deaeration under Ar atmosphere). Blank solvent corrections were made before recording the spectra of each sample and all measurements were recorded under gentle stirring. All measurements were performed in PBS solution testing different ratios of hSA:hemin and hSA:hemin:PFOA. The final concentrations were 10 μM hemin, 2 μM hSA and 100 μM PFOA for the spectra in Figure 1**A**. For the kinetic study, a fixed volume of hSA or hSA:PFOA solution was added to the hemin solution (final concentration of 1 μM hemin, 1 μM hSA and PFOA/PFOS concentrations ranging from 1 to 100 μM) and equilibrated for five minutes (300 s) while recording a spectrum every second. Data were collected within the wavelength range 250–900 nm, considering that the primary region of interest is the Soret band of porphyrin centred at about 400 nm [29]. All spectra were treated with Orange and Origin 2018 software.

2.3. Electrochemical characterisation of hemin

All electrochemical measurements were carried out using a Metrohm Autolab potentiostat/galvanostat (PGSTAT 302 N, Metrohm Autolab) controlled by NOVA 2.1 software. A standard three-electrode configuration was used, consisting of a glassy carbon electrode (GCE) as working electrode, a platinum wire as counter electrode and a saturated calomel electrode (SCE) as reference electrode (all the potentials reported in this work are *vs* the SCE, unless stated otherwise). The GCEs were polished using alumina slurries (0.3, 0.1 and 0.05 μm) with intermediate rinsing steps using MilliQ water. A hemin stock solution (5 mM) was prepared in 100 mM NaOH (since the solubility of porphyrins increases at basic pH) and diluted to 5 μM in 5 mL of PBS solution at pH 7.4. The solutions were degassed with Ar for 20 min before starting the measurements, and throughout the measurements, an Ar blanket was kept above the measuring solution. A negative initial scan polarity was used for all voltammograms recorded because, in these working conditions, the reduction of hemin Fe^{3+} to Fe^{2+} is the first process occurring, so the addition of electrons to the system in the initial scan step (negative polarity) facilitates the reduction. Cyclic voltammetry (CV) was performed in the potential window between −1.00 V and + 0.20 V, with a starting potential of −0.01 V, at different scan rates ranging from 0.01 to 100 V s^{-1}. Square wave voltammetry (SWV) was carried out at 10–20 Hz with a pulse amplitude of 0.0025 V and a step potential of 0.001 V going from 0.00 V to −1.00 V (*forward scan*) and vice versa (*backward scan*). All measurements were performed at room temperature. For the study of hemin's electron transfer kinetics, a hemin concentration of 0.5 mM was used.

2.4. Electrochemical assay for PFOA monitoring in solution

These measurements were performed using the electrochemical setup and working conditions described in Section 2.3. Prior to performing the assay, PFOA spiked samples with concentrations ranging from 10 to 90 μM were prepared in PBS solution at room temperature. Then, hSA was added to each sample to a final concentration of 5 μM. The samples were incubated for 15 min at + 4 °C. This step was followed by the addition of the redox active probe, hemin, in solution to a final concentration of 5 μM (1:1, hSA:hemin). The mixture was gently stirred for 30 s prior to record the SWV scan. As control experiments, PFOA samples without hSA were considered. The SWV signal recorded in 5 μM hemin in buffer solution was measured as the blank.

3. Results and discussion

3.1. Spectroscopic characterisation of Haem:hSA complexes

Hemin:hSA complexes were studied in the presence and absence of PFOA using UV–Vis spectroscopy to confirm the formation of the complexes. The changes in the absorption spectra during the titration of hemin with hSA and hSA:PFOA were analysed, considering the shifts in hemin characteristic bands, especially the Soret band. The macrocycle of porphyrin-based compounds, such as hemin (see Figure 1**S**), has a fully conjugated aromatic π-electron system which is responsible for: *i)* the characteristic strong absorption bands in near UV, namely Soret or B band (around 400 nm) and *ii)* the lower bands in the visible region, namely α and β Q band (at about 490–650 nm). These electronic transitions were assigned using the four-orbital model of Gouteman, as described by Dayer *et al.* [40]. It is worth noting that the formation of porphyrin-protein complexes influences the electronic transitions of both hemin and hSA, shifting their characteristic absorption bands. In Figure 1**A,** the spectrum of a 10 μM hemin solution (see spectrum *H*, *red line*) shows a low intensity band around 265 nm, a band with a wavelength of maximum absorbance (λ_{max}) of 350 nm, a broad Soret band with a λ_{max} of 385 nm and a large, undefined band from 550 to 650 nm. The formation of hemin dimers and the occurrence of vibrionic coupling phenomena can explain the broadening of UV bands and the complete overlap of the band at 350 nm with the Soret ones. Aggregation processes are responsible for the overlap of α and β Q band in the region from 550 to 650 nm. Because of their lower intensities, Q bands will not be further considered in this screening study and only the region from 250 to 550 nm will be considered to evaluate the changes in hemin:hSA complexes (see inset in Figure 1**A**). Indeed, it was observed that the addition of hSA to the hemin solution with a hemin:hSA ratio of 5:1 (see *H:hSA spectrum*, *blue navy line*, Figure 1**A**) is followed by a bathochromic shift (*red shift)* of the Soret band and the appearance of another well-defined band with λ_{max} at 280 nm. This latter is ascribed to the intrinsic fluorescence of proteins determined by the presence of aromatic amino acids (such as tryptophan, tyrosine and phenylalanine) and confirms that hSA is in its native state. A red shift of about 15 nm was observed and ascribed to the formation of the hemin:SA complex [41,42]. Even in the presence of PFOA, a meaningful red shift was recorded (see *H-has:PFOA* spectrum, light blue, Figure 1**A**). It is worth noting that the fluorinated compound was incubated with hSA (1:50 ratio) for 15 min prior to performing the analysis ensuring the formation of the PFOA:hSA complex before adding hemin. The results confirmed the formation of the hemin:hSA complex even in presence of PFOA. As negative controls, a hemin:PFOA mixture (1:10 ratio) and a PFOA solution were tested (*H:PFOA, orange* and *H*, *grey* Figure 1**A**) showing that PFOA does not affect the position of the typical Soret absorption band of hemin because no significant changes in the band λ_{max} were recorded and that PFOA itself does not give any absorbance.

The kinetics of hemin binding to hSA and hSA:PFOA were followed by recording the absorbance at a fixed wavelength of 396 nm, which corresponds to the maximum of the complex band, over a time frame of 300 s starting from the addition of hSA in the hemin solution (t_0). The absorbance *vs* time plots recorded at different PFOA ratios (exemplified in **Figure S3**) are characterised by a consistent trend: a first linear

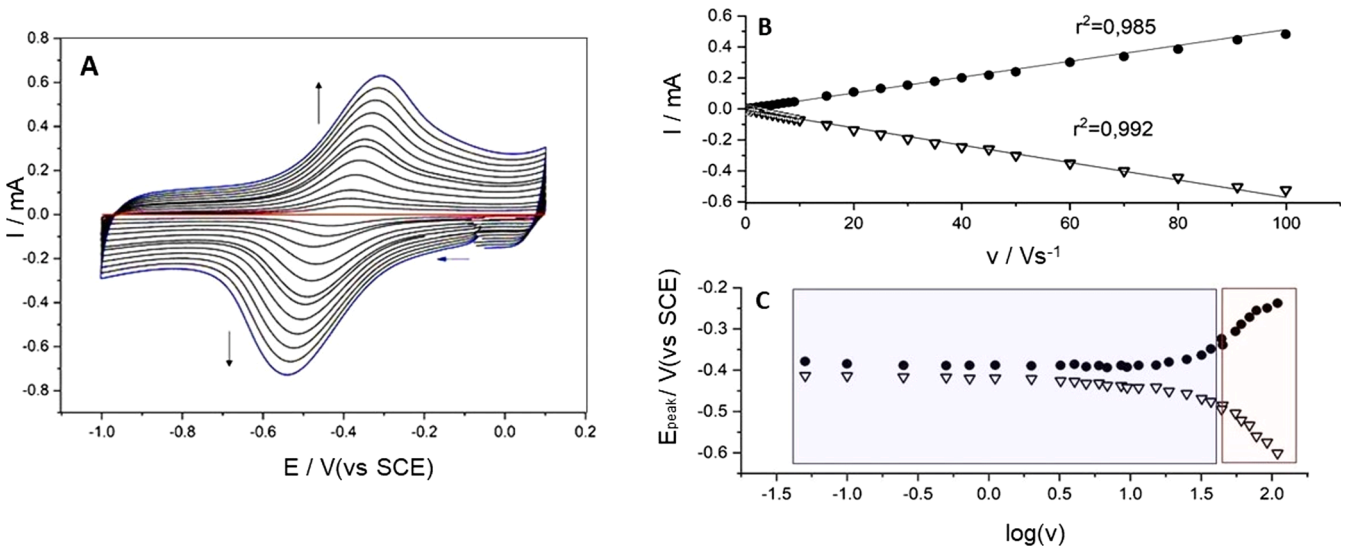

Figure 2. (**A**) Overlap of the cyclic voltammograms recorded in 0.5 mM of hemin in PBS solution pH 7.4 at increasing scan rates (from red to blue: 0.01, 0.05, 0.1, 0.25, 0.5, 0.75, 1.0, 2.0, 3.0, 4.0, 5.0, 6.0, 7.0, 8.0, 9.0, 10.0, then with 5 V s^{-1} increments until 50 V s^{-1} and with 10 V s^{-1} increments until 100 V s^{-1} in blue); (**B**) Linear dependence of the cathodic (triangle) and anodic (dots) peak potential values on the scan rate with r^2 coefficient values; (**C**) Laviron trumpet plot showing the dependence of the cathodic (triangle) and anodic (dots) peak potential values on the logarithm of the scan rate. The purple box indicates the region in which $\Delta E <$ 200/n mV and the red box indicates the data region in which the $\Delta E >$ 200/n mV condition is verified.

increase (0–30 s) of the signal that goes toward saturation for t > 30 s. The data from the linear region were analysed using a first order kinetic reaction model. The kinetic constants (k_s) were normalised against the one of hemin:hSA ($k_{s\ hSA}$) to evaluate the changes in the complex formation kinetics when varying the concentration of PFOA. In Figure 1**B**, a comparison of the k_s / $k_{s\ hSA}$ values *vs* the different PFOA:hSA:hemin ratios is reported. The results show a decrease in the k_s /ks_{hSA} upon increasing concentrations of PFOA. These findings suggest that the formation of the PFOA:hSA complex and the presence of an excess of PFOA in solution are lowering the kinetics of hemin binding to hSA. The 1:1:1 PFOA:hSA:hemin ratio (1 μM PFOA) was found to lead to a decrease in the hemin binding kinetics of about 35%. Concerning the λ_{max}, blue shifts of 2–6 nm were observed for PFOA:hSA:hemin ratios higher than 25:1:1 (25 μM PFOA). These findings confirmed that PFOA, as well as WAR and IBU, can affect the kinetics of hemin binding to hSA [30]. The same experiment was performed using another perfluorinated compound, namely PFOS, instead of PFOA. This control experiment aimed at proving that the reduction in the kinetic constant is associated to the specific ability of PFOA to bind albumin's pocket FA7 and alter the conformation of FA1 where hemin binds [34]. Here, the PFOS was selected because it has the same chain length of PFOA but shows a different binding mode to hSA [35]. PFOS:hSA complexes differ from PFOA:hSA ones in stoichiometry and binding sites [35].

As expected, in the presence of PFOS no meaningful changes in the k_s / $k_{s\ hSA}$ were observed upon increased PFOS ratios, as summarised in Figure 1**B**. Overall, the UV–Vis study confirmed the formation of stable hemin:hSA complexes and the influence of PFOA on hemin:hSA complex formation. The multiple equilibria at stake (hemin:hSA, hSA:PFOA, hemin:hSA:PFOA) should be further considered in the design of an electrochemical strategy for PFOA monitoring. However, prior to applying hemin as a probe in our sensing strategy, we need to characterise, *via* voltammetric techniques, its electrochemical behaviour and electron transfer (ET) kinetics in the described working conditions. It is worth noting that such working conditions (see **Section 2.3**) were selected aiming at assuring the stability of hSA, but are not optimal for hemin, which is poorly soluble in aqueous media.

3.2. Electrochemical study of haem

The cyclic voltammograms of 0.5 mM hemin in PBS pH 7.4 under an Ar atmosphere show the reversibility of the Fe^{2+}-Fe^{3+} redox couple with an $E_{p1/2}$ of about −0.56 V and a ΔE of around 100 mV at 0.100 V s^{-1} (see Figure 2**A**). The one-electron, reversible nature of the redox process, previously reported, was clearly observed even in these working conditions [28]. To further characterise this potential redox probe and determine its ET rate constant (k_s), an extensive scan rate study was performed by CV in the range between 0.010 V s^{-1} and 100 V s^{-1} (see Figure 2**A**). The peak separation is increasing with the scan rate: a linear dependence of the cathodic and anodic peak current intensities (I_p) with the scan rate (v) was observed with $r^2 > 0.99$ (see Figure 2**B**). For the application of Laviron formalism, the electrochemical process is required to be diffusionless and consistent with the Butler-Volmer model [38,43]. This last requirement can be verified by checking the linearity of Ep *vs* log v dependence at high scan rates.

Once the requirements were verified, the characteristic *trumpet* plot reported in Figure 2**B** was elaborated by plotting the cathodic and anodic peak potentials *vs* the logarithm of the scan rate (log v). Afterwards, we applied the Laviron formalism (calculations described in **Section S1**, Supporting Information) to calculate the k_s values. Considering that most E_p values present a $\Delta E <$ 200/n mV, it was possible to estimate a k_s value for the ET of hemin of 15.5 ± 2.5 s^{-1}. The k_s was also calculated for the E_p values, fulfilling condition $\Delta E >$ 200/n obtaining a value of 19.4 ± 7.3 s^{-1}. In general, the k_s calculated from the trumpet plot by considering $\Delta E >$ 200/n values is higher than the one extrapolated using **Equation 3** (**Section S1**, Supporting Information), as previously reported [44]. In this frame, both k_s values were considered consistent, and the hemin redox probe was proven to be applicable in the following working conditions because of its k_s values.

3.3. Towards albumin-based PFOA direct sensing

A proof-of-concept study, aimed at verifying hemin's applicability in PFOA sensing, was carried out. On one hand, we expected to observe a current variation after the addition of hSA to the working solution because the hemin:hSA complex will be easily formed and the ET of the hemin iron centre will be partially hindered by the hSA's hydrophobic pocket. When hSA is loaded with PFOA prior to adding hSA to the working solution, hSA:hemin binding will be affected by the presence of PFOA and the electrochemical signals of hemin will possibly decrease less than with hSA alone. Naturally, these equilibria can be influenced

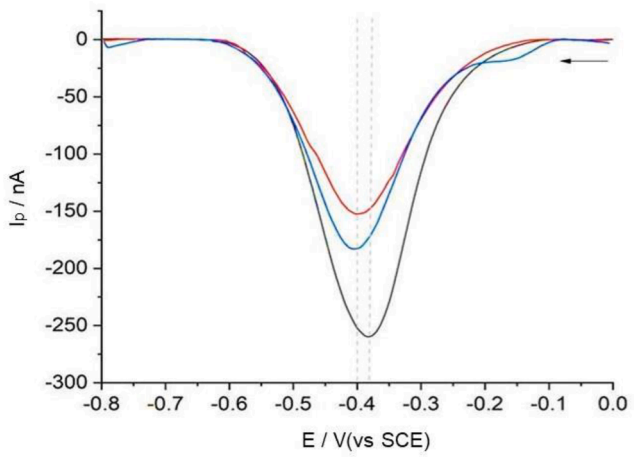

Figure 3. Square wave voltammograms of hemin (black curve), hemin:hSA (red curve) and hemin:hSA:PFOA (ratio 1:1:50; light blue curve); the shift in the Ep values is shown by the vertical dotted lines in grey.

by other phenomena, but those were not addressed in this study. The mentioned hypothesis was investigated by performing a CV and SVW study using a fixed hemin concentration of 5 μM and considering different hemin:hSA and hSA:PFOA ratios.

PFOA will decrease hemin's availability, which can be followed by tracking the changes in the hemin faradic signal (especially in terms of current intensities). Figure 3 provides an example of hemin, hemin:hSA and hemin:hSA:PFOA voltammograms recorded via SWV. Hemin presents a unique, symmetric cathodic peak with an E_p of −0.383 V that shifts to −0.404 V when hSA is added with a 1:1 hemin:hSA ratio. This shift towards higher potentials ($\Delta E_p = 20$ mV) is followed by a decrease in the I_p of hemin of 41%. Both the shift in E_p and the current decrease can be ascribed to the hemin:hSA complex formation, which has previously been shown to influence albumin's intrinsic fluorescence [29]. In our case, it leads to a decrease in the ET rate.

When, instead of hSA, hSA:PFOA is added to the working solution (ratio 1:1:50, Figure 3) a current decrement of about 30% is recorded compared to hemin alone. This lower decrease in hemin I_p in the presence of PFOA is possibly due to the slower kinetics of hemin:hSA complex formation when PFOA is absent. Indeed, PFOA, which was previously loaded in hSA hydrophobic pockets, is expected to induce an allosteric change in hSA FA1, hampering hemin binding to the hSA:PFOA complex and leading to a major availability of free hemin compared to hSA alone. It is worth noting that PFOA shows no electroactive behaviour in the potential window considered in this study [37,44,45].

The influence of increasing PFOA:hSA ratios on the hemin voltammetric response was explored in the range between 1:1 and 1:100. The voltammograms in Figure 4**A** show an increase in hemin I_p current at increasing ratios of PFOA (going from **a**, 1:10, to **f**, 1:90). All hemin I_p values recorded in the presence of hSA and hSA:PFOA were normalised towards the I_p value of hemin alone (*black line* in Figure 4**A**). The normalised values of hemin:hSA:PFOA at different PFOA concentrations are presented in Figure 4**B**. We can observe that, with PFOA concentrations lower than 20 μM, the ΔI_p is lower than 0.10, while for concentrations higher than 40 μM the variation of this parameter is significant and follows a linear trend (details in **Figure S4**). The hemin I_p current decreases, going from 30% to 16.9% between 40 and 100 μM of PFOA. If, instead of PFOA, PFOS is used, no meaningful changes in the peak potential and current intensity were observed. These findings can be explained by considering that the binding mechanism of PFOS to hSA differs from that of PFOA [34,36,46] and the complex formed is not expected to undergo any conformational changes in hemin site FA1. This negative control experiment further supports our data interpretation.

These results suggest the possibility of, indirectly, monitoring increasing PFOA concentrations by following the changes in hemin's reduction peak in the presence of the hSA:PFOA complex. To draw a sensing strategy from this proof-of-concept study, we need to consider that: *i)* PFOA contaminated samples need to be incubated first with hSA (to assure the hSA:PFOA complex formation) and then with the hemin redox probe; and *ii)* only high ratios of hSA:PFOA will be detectable.

Overall, the described data suggest the possibility of combining commercially available electroactive labels, such as hemin, to hSA-based sensing strategies for nonelectroactive contaminants.

4. Conclusions

Evaluating hemin's applicability as a probe in PFOA voltammetric sensing allowed us to further investigate the possible connections between pharmacokinetic studies and biosensing design. Indeed, well-known conformational changes in albumin pockets caused by certain drugs that affect haem (hemin) binding might occur even when another molecule, PFOA in this case, binds to the same sites. Aiming to verify this

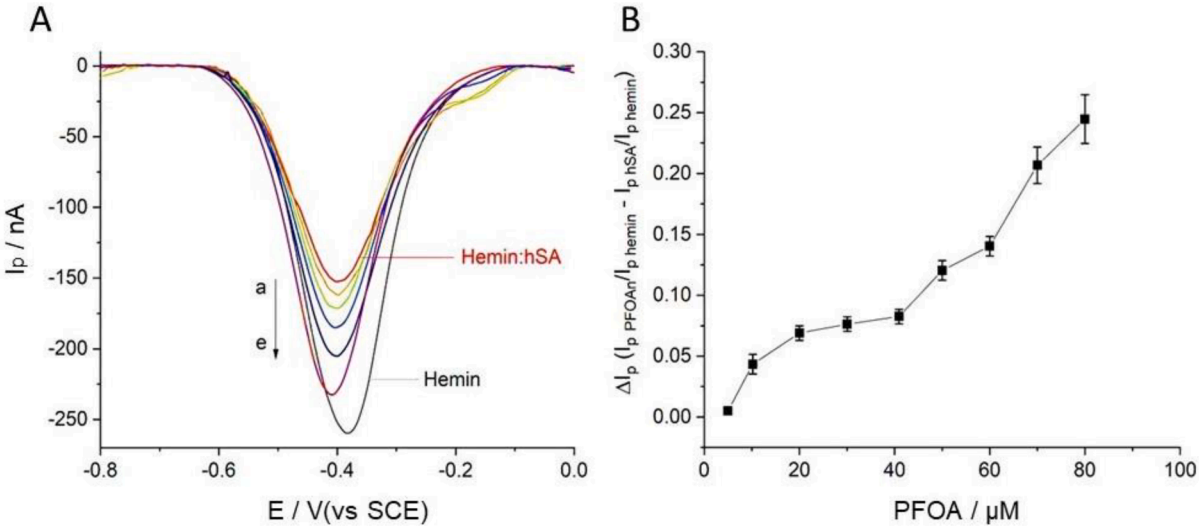

Figure 4. (**A**) Square wave voltammograms of hemin (black line), hemin:hSA (red line) and hemin:hSA:PFOA at increasing PFOA ratios: from 1:1:10 (**a**) to 1:1:90 (**f**); (**B**) Plot of the normalised values ($I_{p\text{-PFOA}}/I_{p\text{-hemin}}$ - $I_{p\text{-hSA}}/I_{p\text{-hemin}}$) of hemin:hSA:PFOA at different PFOA concentrations. All measurements were carried out in triplicates and the average values with the associated errors are presented.

hypothesis, a UV–Vis study was carried out. The hemin-hSA complex kinetic results were impacted by the presence of the contaminant. Therefore, it was possible to move forward and try to follow these variations through electrochemistry, considering the changes in the voltammetric behaviour of hemin. The preliminary data confirmed the possibility of correlating the changes in the intensity of the hemin reduction peak with increasing PFOA:hSA ratios. It is worth noting that the ratios considered here were relatively high compared to those of real samples. Nevertheless, for this preliminary study, it was necessary to evaluate the magnitude of the signal changes in the presence of relatively high ratios of PFAS. Naturally, this is only a first step to investigate the possibility of designing analytical devices for PFAS detection based on hSA and hemin.

Even though PFOA sensing with a hemin probe seems difficult to combine with a real analytical context (oxygen-free conditions are difficult to obtain in-situ with portable devices), the development of a sensor by combining a nonelectroactive ligand and a bioreceptor with an electroactive probe paves the way for further studies where optimisation of conditions could lead to a sensor that can be applied in real analytical contexts. Therefore, this biosensing strategy could be integrated with protein-based PFAS bioremediation approaches [47] to monitor PFOA levels in treated water. In addition, by engineering albumins, it would be possible to selectively determine multiple PFAS, both long- and short-chain ones [48], using this type of electrochemical assay.

Declaration of Competing Interest

The authors declare that they have no known competing financial interests or personal relationships that could have appeared to influence the work reported in this paper.

Data availability

No data was used for the research described in the article.

Appendix A. Supplementary data

Supplementary data to this article can be found online at https://doi.org/10.1016/j.bioelechem.2023.108428.

References

[1] C.-M. Wu, L.-Y. Lin, Utilization of albumin-based sensor chips for the detection of metal content and characterization of metal–protein interaction by surface plasmon resonance, Sens. Actuators B Chem. 110 (2005) 231–238, https://doi.org/10.1016/j.snb.2005.01.047.

[2] N.U. Amin, H.M. Siddiqi, Y. Kun Lin, Z. Hussain, N. Majeed, Bovine Serum Albumin Protein-Based Liquid Crystal Biosensors for Optical Detection of Toxic Heavy Metals in Water, Sensors 20 (2020), https://doi.org/10.3390/s20010298.

[3] C. He, M. Xie, F. Hong, X. Chai, H. Mi, X. Zhou, L. Fan, Q. Zhang, T. Ngai, J. Liu, A highly sensitive glucose biosensor based on gold nanoparticles/bovine serum albumin/Fe3O4 biocomposite nanoparticles, Electrochim. Acta. 222 (2016) 1709–1715, https://doi.org/10.1016/j.electacta.2016.11.162.

[4] Z. Tang, Y. Fu, Z. Ma, Bovine serum albumin as an effective sensitivity enhancer for peptide-based amperometric biosensor for ultrasensitive detection of prostate specific antigen, Biosens. Bioelectron. 94 (2017) 394–399, https://doi.org/10.1016/j.bios.2017.03.030.

[5] R. Wang, X. Zhou, X. Zhu, C. Yang, L. Liu, H. Shi, Isoelectric Bovine Serum Albumin: Robust Blocking Agent for Enhanced Performance in Optical-Fiber Based DNA Sensing, ACS Sensors 2 (2017) 257–262, https://doi.org/10.1021/acssensors.6b00746.

[6] M.V. Riquelme, H. Zhao, V. Srinivasaraghavan, A. Pruden, P. Vikesland, M. Agah, Optimizing blocking of nonspecific bacterial attachment to impedimetric biosensors, Sens. Bio-Sensing Res. 8 (2016) 47–54, https://doi.org/10.1016/j.sbsr.2016.04.003.

[7] Y.-H. Liu, H.-N. Li, W. Chen, A.-L. Liu, X.-H. Lin, Y.-Z. Chen, Bovine Serum Albumin-Based Probe Carrier Platform for Electrochemical DNA Biosensing, Anal. Chem. 85 (2013) 273–277, https://doi.org/10.1021/ac303397f.

[8] Y. He, Y. Liu, L. Cheng, Y. Yang, B. Qiu, L. Guo, Y. Wang, Z. Lin, G. Hong, Highly Reproducible and Sensitive Electrochemiluminescence Biosensors for HPV Detection Based on Bovine Serum Albumin Carrier Platforms and Hyperbranched Rolling Circle Amplification, ACS Appl. Mater. Interfaces 13 (2021) 298–305, https://doi.org/10.1021/acsami.0c20742.

[9] A. Kłos-Witkowska, B. Akhmetov, N. Zhumangalieva, V. Karpinskyi, T. Gancarczyk, Bovine Serum Albumin stability in the context of biosensors, in: 2016 16th Int. Conf. Control. Autom. Syst., Korea (South), 2016, 976–980. https://doi.org/10.1109/ICCAS.2016.7832427.

[10] E. Zor, I. Hatay Patir, H. Bingol, M. Ersoz, An electrochemical biosensor based on human serum albumin/graphene oxide/3-aminopropyltriethoxysilane modified ITO electrode for the enantioselective discrimination of D- and L-tryptophan, Biosens. Bioelectron. 42 (2013) 321–325, https://doi.org/10.1016/j.bios.2012.10.068.

[11] Y. Li, R. Han, M. Chen, X. Yang, Y. Zhan, L. Wang, X. Luo, Electrochemical biosensor with enhanced antifouling capability based on amyloid-like bovine serum albumin and a conducting polymer for ultrasensitive detection of proteins in human serum, Anal. Chem. 93 (2021) 14351–14357, https://doi.org/10.1021/acs.analchem.1c04153.

[12] H. Yang, Q. Hou, C. Ding, Denatured bovine serum albumin hydrogel–based electrochemical biosensors for detection of IgG, Microchim. Acta. 189 (2022) 400, https://doi.org/10.1007/s00604-022-05499-9.

[13] T.H.V. Kumar, A.K. Sundramoorthy, Electrochemical biosensor for methyl parathion based on single-walled carbon nanotube/glutaraldehyde crosslinked acetylcholinesterase-wrapped bovine serum albumin nanocomposites, Anal. Chim. Acta. 1074 (2019) 131–141, https://doi.org/10.1016/j.aca.2019.05.011.

[14] V. Shumyantseva, T. Bulko, A. Kuzikov, R. Masamrekh, A. Archakov, Analysis of l-tyrosine based on electrocatalytic oxidative reactions via screen-printed electrodes modified with multi-walled carbon nanotubes and nanosized titanium oxide (TiO2), Amino Acids 50 (2018) 823–829, https://doi.org/10.1007/s00726-018-2557-z.

[15] E.V. Suprun, M.S. Zharkova, G.E. Morozevich, A.V. Veselovsky, V. V. Shumyantseva, A.I. Archakov, Analysis of Redox Activity of Proteins on the Carbon Screen Printed Electrodes, Electroanalysis 25 (2013) 2109–2116, https://doi.org/10.1002/elan.201300248.

[16] G. Moro, K. De Wael, L.M. Moretto, Challenges in the electrochemical (bio)sensing of nonelectroactive food and environmental contaminants, Curr. Opin. Electrochem. 16 (2019) 57–65, https://doi.org/10.1016/j.coelec.2019.04.019.

[17] H. Shinohara, H. Kuramitz, K. Sugawara, Design of an electroactive peptide probe for sensing of a protein, Anal. Chim. Acta. 890 (2015) 143–149, https://doi.org/10.1016/j.aca.2015.07.052.

[18] R.S. Tieman, L.A. Coury, J.R. Kirchhoff, W.R. Heineman, The electrochemistry of hemin in dimethylsulfoxide, J. Electroanal. Chem. 281 (1990) 133–145, https://doi.org/10.1016/S0022-0728(90)87035.

[19] M. Paoli, B.F. Anderson, H.M. Baker, W.T. Morgan, A. Smith, E.N. Baker, Crystal structure of hemopexin reveals a novel high-affinity heme site formed between two β-propeller domains, Nat. Struct. Biol. 6 (1999) 926–931, https://doi.org/10.1038/13294.

[20] P.A. Adams, M.C. Berman, Kinetics and mechanism of the interaction between human serum albumin and monomeric haemin, Biochem. J. 191 (1980) 95–102, https://doi.org/10.1042/bj1910095.

[21] V.V. Shumyantseva, T.V. Bulko, E.V. Suprun, A.V. Kuzikov, L.E. Agafonova, A. I. Archakov, Electrochemical methods in biomedical studies, Biochem. Suppl. Ser. B Biomed. Chem. 9 (2015) 228–243, https://doi.org/10.1134/S1990750815030087.

[22] V.V. Shumyantseva, T.V. Bulko, A.G. Zimin, V.Y. Uvarov, A.I. Archakov, Design of an artificial hemoprotein based on human serum albumin, Biochem. Mol. Biol. Int. 39 (1996) 503–510, https://doi.org/10.1080/15216549600201551.

[23] M. Rosenfeld, D.M. Surgenor, Methemalbumin: interaction between human serum albumin and ferriprotoporphyrin IX, J. Biol. Chem. 183 (1950) 663–677, https://doi.org/10.1016/S0021-9258(19)51193-0.

[24] A.V. Solomonov, E.V. Rumyantsev, E.V. Antina, Serum albumin and its bilirubin complex as drug-carrier proteins for water-soluble porphyrin: a spectroscopic study, Monatsh. Chem. Mon. 144 (2013) 1743–1749, https://doi.org/10.1007/s00706-013-1062-z.

[25] T. Komatsu, N. Ohmichi, P.A. Zunszain, S. Curry, E. Tsuchida, Dioxygenation of human serum albumin having a prosthetic heme group in a tailor-made heme pocket, J. Am. Chem. Soc. 126 (2004) 14304–14305, https://doi.org/10.1021/ja046022t.

[26] S. Curry, Beyond expansion: structural studies on the transport roles of human serum albumin, Vox Sang. 83 (2002) 315–319, https://doi.org/10.1111/j.1423-0410.2002.tb05326.x.

[27] P.A. Zunszain, J. Ghuman, T. Komatsu, E. Tsuchida, S. Curry, Crystal structural analysis of human serum albumin complexed with hemin and fatty acid, 9 (2003) 6 https://doi.org/10.1186/1472-6807-3-6.

[28] R.N. Samajdar, D. Manogaran, S. Yashonath, A.J. Bhattacharyya, Using Porphyrin-Amino Acid Pairs to Model the Electrochemistry of of Heme Proteins: Experimental and Theoretical Investigations, Phys. Chem. Chem. Phys. 20 (2018) 10018–10029, https://doi.org/10.1039/C8CP00605A.

[29] M. Makarska-Bialokoz, Interactions of hemin with bovine serum albumin and human hemoglobin: A fluorescence quenching study, Spectrochim. Acta - Part A Mol. Biomol. Spectrosc. 193 (2018) 23–32, https://doi.org/10.1016/j.saa.2017.11.063.

[30] S. Baroni, M. Mattu, A. Vannini, R. Cipollone, S. Aime, P. Ascenzi, M. Fasano, Effect of ibuprofen and warfarin on the allosteric properties of haem – human serum albumin, Eur. J. Biochem. 268 (2001) 6214–6220, https://doi.org/10.1046/j.0014-2956.2001.02569.x.

[31] I. Fitos, J. Visy, J. Kardos, Stereoselective kinetics of warfarin binding to human serum albumin: Effect of an allosteric interaction, Chirality 14 (2002) 442–448, https://doi.org/10.1002/chir.10113.

[32] I. Petitpas, A.A. Bhattacharya, S. Twine, M. East, S. Curry, Crystal structure analysis of warfarin binding to human serum albumin. Anatomy of drug site I, J. Biol. Chem. 276 (2001) 22804–22809. https://doi.org/10.1074/jbc.M100575200.
[33] J. Wilting, W.F. van der Giesen, L.H. Janssen, M.M. Weideman, M. Otagiri, J. H. Perrin, The effect of human albumin conformation on the binding of warfarin. The dependence of the binding of warfarin to human serum albumin on the hydrogen, calcium, and chloride ion concentrations as studied by circular dichroism, fluorescence, and equilibrium dialysis, J. Biol. Chem. 255 (1980) 3032–3037.
[34] M. Salvalaglio, I. Muscionico, C. Cavallotti, Determination of energies and sites of binding of PFOA and PFOS to human serum albumin, J. Phys. Chem. B 114 (2010) 14860–14874, https://doi.org/10.1021/jp106584b.
[35] L. Maso, M. Trande, S. Liberi, G. Moro, E. Daems, S. Linciano, F. Sobott, S. Covaceuszach, A. Cassetta, S. Fasolato, L.M. Moretto, K. De Wael, L. Cendron, A. Angelini, Unveiling the binding mode of perfluorooctanoic acid to human serum albumin, Protein Sci. 30 (2021) 830–841, https://doi.org/10.1002/pro.4036.
[36] E. Daems, G. Moro, H. Berghmans, L.M. Moretto, S. Dewilde, A. Angelini, F. Sobott, K. De Wael, Native mass spectrometry for the design and selection of protein bioreceptors for perfluorinated compounds, Analyst 146 (2021) 2065–2073, https://doi.org/10.1039/D0AN02005B.
[37] G. Moro, F. Bottari, S. Liberi, S. Covaceuszach, A. Cassetta, A. Angelini, K. De Wael, L.M. Moretto, Covalent immobilization of delipidated human serum albumin on poly(pyrrole-2-carboxylic) acid film for the impedimetric detection of perfluorooctanoic acid, Bioelectrochemistry 134 (2020), 107540, https://doi.org/10.1016/j.bioelechem.2020.107540.
[38] E. Laviron, General expression of the linear potential sweep voltrammogram in the case of diffusionless electrochemical systems, J. Electroanal. Chem. 101 (1979) 19–28, https://doi.org/10.1016/S0022-0728(79)80075-3.
[39] S. Liberi, S. Linciano, G. Moro, L. De Toni, L. Cendron, A. Angelini, Structural Analysis of Human Serum Albumin in Complex with the Fibrate Drug Gemfibrozil, Int. J. Mol. Sci. 23 (2022) 1769, https://doi.org/10.3390/ijms23031769.
[40] M.R. Dayer, A.A. Moosavi-movahedi, M.S. Dayer, Band Assignment in Hemoglobin Porphyrin Ring Spectrum : Using Four- Orbital Model of Gouterman, 17 (2010) 473–479. https://doi.org/10.2174/092986610790963645.
[41] N. Nanzyo, S. Sano, Type c Ferri- and Ferrohemochrome Formation between Hemin c, Amino Acids, and Peptides, J. Biol. Chem. 243 (1968) 3431–3440, https://doi.org/10.1016/S0021-9258(18)93327-2.
[42] D.-T.-Y. Chiu, J. Van Den Berg, F.A. Kuypers, I.-J. Hung, J.-S. Wei, T.-Z. Liu, Correlation of membrane lipid peroxidation with oxidation of hemoglobin variants: Possibly related to the rates of hemin release, Free Radic. Biol. Med. 21 (1996) 89–95, https://doi.org/10.1016/0891-5849(96)00035-4.
[43] R. Campos, E.E. Ferapontova, Electrochemistry of weakly adsorbed species: Voltammetric analysis of electron transfer between gold electrodes and Ru hexamine electrostatically interacting with DNA duplexes, Electrochim. Acta. 126 (2014) 151–157, https://doi.org/10.1016/j.electacta.2013.07.083.
[44] G. Moro, D. Cristofori, F. Bottari, E. Cattaruzza, K. De Wael, L.M. Moretto, Redesigning an electrochemical MIP sensor for PFOS: Practicalities and pitfalls, Sensors 19 (2019), https://doi.org/10.3390/s19204433.
[45] N. Karimian, A.M. Stortini, L.M. Moretto, C. Costantino, S. Bogialli, P. Ugo, Electrochemosensor for Trace Analysis of Perfluorooctanesulfonate in Water Based on a Molecularly Imprinted Poly(o-phenylenediamine) Polymer, ACS Sensors 3 (2018) 1291–1298, https://doi.org/10.1021/acssensors.8b00154.
[46] Q. Chi, Z. Li, J. Huang, J. Ma, X. Wang, Interactions of perfluorooctanoic acid and perfluorooctanesulfonic acid with serum albumins by native mass spectrometry, fluorescence and molecular docking, Chemosphere 198 (2018) 442–449, https://doi.org/10.1016/j.chemosphere.2018.01.152.
[47] E.T. Hernandez, B. Koo, L.E. Sofen, R. Amin, R.K. Togashi, A.I. Lall, D.J. Gisch, B. J. Kern, M.A. Rickard, M.B. Francis, Proteins as adsorbents for PFAS removal from water, Environ. Sci. Water Res. Technol. 8 (2022) 1188–1194, https://doi.org/10.1039/D1EW00501D.
[48] G. Moro, S. Liberi, F. Vascon, S. Linciano, S. De Felice, S. Fasolato, C. Foresta, L. De Toni, A. Di Nisio, L. Cendron, A. Angelini, Investigation of the Interaction between Human Serum Albumin and Branched Short-Chain Perfluoroalkyl Compounds, Chem. Res. Toxicol. 35 (2022) 2049–2058, https://doi.org/10.1021/acs.chemrestox.2c00211.